J Mater Sci (2009) 44:3015–3019
DOI 10.1007/s10853-009-3374-2

Preparation and tunable photoluminescence of alloyed CdS_xSe_{1-x} nanorods

Chao Yang · Xiaochong Zhou · Longyan Wang ·
Xike Tian · Yanxin Wang · Zhenbang Pi

Received: 20 November 2008 / Accepted: 26 February 2009 / Published online: 13 April 2009

Abstract Ternary alloys of CdS_xSe_{1-x} nanorods have been synthesized by the thermal treatment of Cd^{2+} dispersed polyethylene glycol 2000 gel (PEG2000) with ethylenediamine solution of sulfur and selenium in a sealed system at 180 °C for 24 h, during which the proportion between S and Se in the nanorods was controlled by the ratios of every starting material to each other. The alloyed ternary CdS_xSe_{1-x} nanorods are highly crystalline without any other phase. The optical property these nanorods could be manipulated by modulating the composition of S and Se.

Introduction

The success of compound semiconductors in optoelectronics and integrated circuits is largely attributed to the capability of engineering through composition modulation. For devices in nanoelectronics and nanophotonics, it is very important to fabricate materials with continuously tunable physical properties. During the past few years, extensive attention has been devoted to tune the band gap of the 1D nanostructure through the quantum confinement effect [1–3]. However, progress in this field only gives the ability to generate 1D nanostructure with diameters in a limited range, in which the quantum confinement effect is not prominent. As such, the diameter tuning of electronic, optical, and magnetic properties may cause problems in many applications [4–6]. Whereas, the constituent stoichiometries tuning of band gaps and then their optical emissions has shown a large advance in semiconductor nanostructures [7–12].

As one of the most important II–VI group semiconductors, CdS_xSe_{1-x}, with some unique properties, has large potential application in solar cells, photovoltaic devices, light-emitting devices (LED) [10, 11, 13]. Recently, CdS_xSe_{1-x} has been applied in environmental sensors and infrared photodetector [14, 15]. In this article, we present a class of alloyed ternary CdS_xSe_{1-x} nanorods with continuous tuning of the band gap through composition modulation. The alloyed nanorods were prepared via a solvothermal treatment route. Ethylenediamine was adopted as the reaction medium, and PEG2000 was applied as the polymer-controller matrix. The ratio of S to Se in the nanorods was controlled by the relative amounts of the starting materials. Optical measurements indicate that the band gaps of these nanorods have been continuously tuned from 1.75 eV (CdSe) to 2.44 eV (CdS).

Experimental section

All the chemical reagents used in this experiment were of analytical grade and used with further purification. A typical series of the starting materials with molar ratios Se to (Se + S) in the solutions varied as 0, 0.2, 0.4, 0.6, 0.8, and 1 were used to obtain different x for $CdS_{1-x}Se_x$ nanorods. For

C. Yang · X. Zhou · L. Wang · X. Tian (✉) · Z. Pi
Faculty of Material Science and Chemistry Engineering,
China University of Geosciences, Wuhan 430074,
People's Republic of China
e-mail: xktian@cug.edu.cn

C. Yang · Y. Wang
School of Environmental Studies, China University
of Geosciences, Wuhan 430074, People's Republic of China

example, in the preparation of a bath with a Se/(S + Se) molar ratio of 0.4, 3.08 g (0.01 mol) of $Cd(NO_3)_2 \cdot 4H_2O$ were dissolved into 15.0 g polyethylene glycol 2000 gel (PEG2000, 5.0 g; deionized water, 10.0 g). The solution was stirred at room temperature for 5 h in order to achieve good dispersion of Cd^{2+} in the polymer matrix. Then it was dehydrated at 70 °C to get the polymer gel. An aliquot of 0.192 g (0.006 mol) S, 0.316 g (0.004 mol) Se, and 5 mL of $N_2H_4H_2O$ were dissolved in 30 mL ethylenediamine, and then, the PEG gel dosed with Cd^{2+} was mix with the ethylenediamine solvent The reactant solution was stirred for 10 min at room temperature and then removed to a stainless steel autoclave with a Teflon liner. The autoclave was kept at 180 °C for 24 h and then cooled to room temperature naturally. After the reaction, the solution was filtered and washed with absolute ethanol and distilled water, dried in air at 80 °C for 4 h. Then continuous crystalline nanorods are obtained at 200 °C annealing.

The phase purity of the as-prepared products was performed by X-ray power diffraction (XRD) using a Philip X'Pert Pro diffractometer with Cu Kα radiation ($\lambda = 1.5406$). Transmission electron microscope (TEM) photographs and selected area electron diffraction patterns were taken on a JEM-100CXII model transmission electron microscope at an accelerating voltage of 200 kV. The photoluminescence (PL) emission was taken on a luminescence spectrophotometer (LS55, Perkin-Elmer). The excitation wavelength was 405 nm and the bandwidths were 10 nm for emission. All optical measurements were carried out at room temperature.

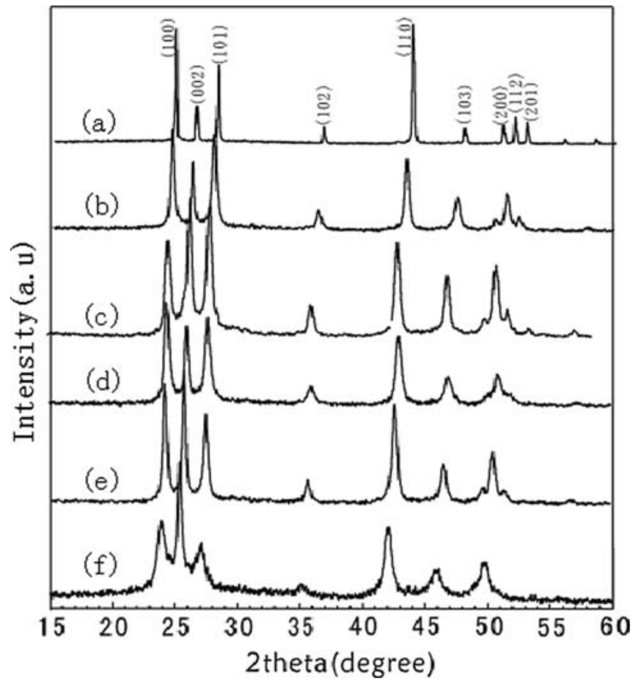

Fig. 1 The normalized X-ray diffraction patterns of several CdS$_x$Se$_{1-x}$ products with different composition (a) CdS, (b) CdS$_{0.8}$Se$_{0.2}$, (c) CdS$_{0.6}$Se$_{0.4}$, (d) CdS$_{0.4}$Se$_{0.6}$, (e) CdS$_{0.2}$Se$_{0.8}$, (f) CdSe

Results and discussion

Figure 1 shows the X-ray diffraction patterns of several representative CdS$_x$Se$_{1-x}$ ($0 \leq x \leq 1$) samples. Curves a and e correspond to the wurtzite CdS and CdSe nanorods, respectively, compared with standard patterns of CdS(JCPDS 41-1049) and CdSe(JCPDS 08-459), respectively. Curves b–d are corresponding to samples synthesized in turn with Se concentration increasing. It is clearly seen that the crystallographic phase of all the samples is in good agreement with that of the typical wurtzite crystals. From curve a to e, the corresponding diffraction peaks shift gradually toward low angles, indicating that the lattice constants of the nanorods increase when the S concentration decreases.

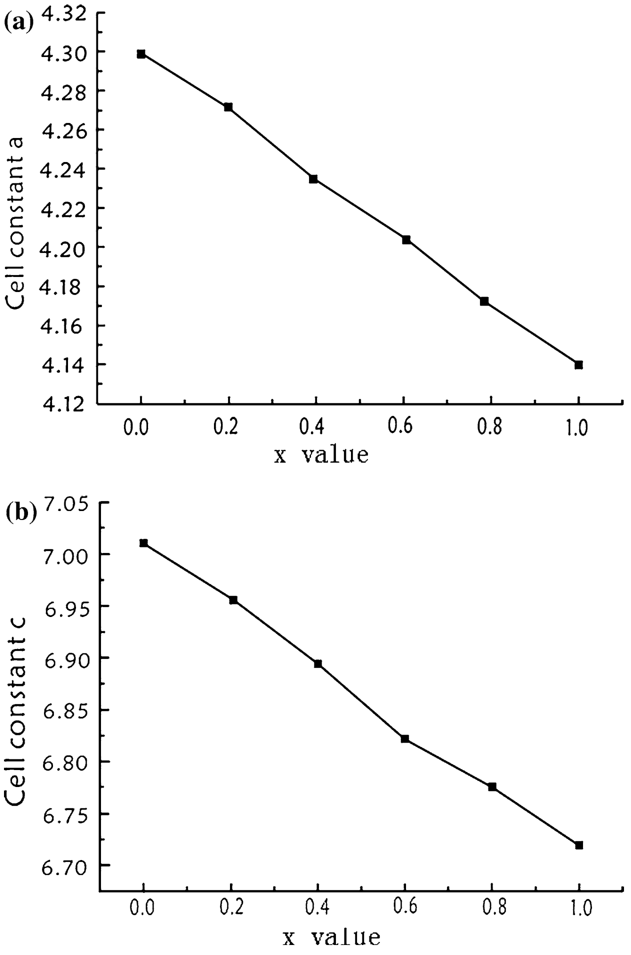

Fig. 2 Calculated cell constant *a* and *c* of the CdS$_x$Se$_{1-x}$ samples with different composition

According to Vegard's law for ternary CdS_xSe_{1-x} compounds [16], the lattice parameters have a linear dependence on the composition x. The cell constants a and c can be calculated according to Eq. 1

$$\frac{1}{d_{hkl}{}^2} = \frac{4}{3}\frac{h^2 + hk + l^2}{a^2} + \frac{l^2}{c^2} \tag{1}$$

where h, k, and l are the Miller indices of the lattice planes and d_{hkl} is the lattice plane distance, which can be determined by X-ray, using the Bragg equation $d_{hkl} = n\lambda/2\sin\theta$, in which n is the refractive. As shown in Fig. 2, the calculated cell constants (dots) obtained comply well with Vegard's rules, which assumes a linear dependence on the composition parameter x as shown in Eq. 2

$$\begin{aligned} a\ CdS_xSe_{1-x} &= x \cdot a\ CdS + (1-x) \cdot a\ CdSe \\ c\ CdS_xSe_{1-x} &= x \cdot c\ CdS + (1-x) \cdot c\ CdSe \end{aligned} \tag{2}$$

This indicated that the real compositions of the CdS_xSe_{1-x} products are in good agreement with the compositions of the reactants. No patterns of impurities or remaining Se were found, indicating the reaction was completed.

TEM images of the CdS_xSe_{1-x} nanostructures with different compositions ($x = 0.2$, 0.5, 0.8) are shown in Fig. 3. It can be seen that the samples are all composed of regular nanorods with the typical diameters of 15–20 nm and length of 100–200 nm. TEM images of CdS($x = 0$) and CdSe($x = 1$) products show that their morphology and size distribution are the same. The selected area electron diffraction pattern confirms the single-crystal quality of the rods, and can be indexed to have a hexagonal structure. The corresponding HR-TEM image further demonstrated a single-crystalline structure with 0.345 nm lattice spacing, corresponding to the (002) interplanar distance of hexagonal CdS_xSe_{1-x}.

Figure 4 gives the normalized PL spectra of the obtained CdS_xSe_{1-x} nanorods recorded at room temperature. Curves a and f are the PL spectra of CdSe and CdS nanorods, and Curves b–e corresponding to the CdS_xSe_{1-x} nanorods with different compositions ($x = 08$, 0.6, 0.4, 0.2), respectively. The PL spectrum of each sample is characterized with two different radioactive bands: the high energies band corresponds to the near band edge (NBE) recombination and the

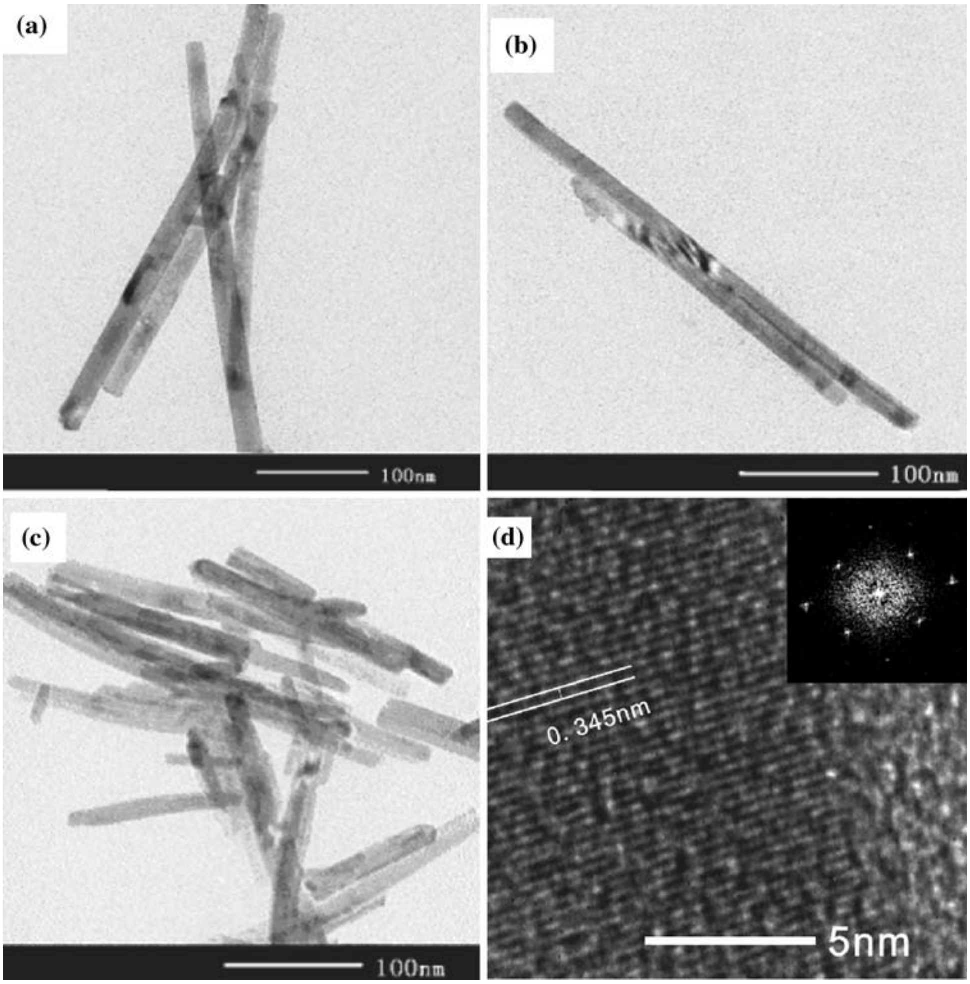

Fig. 3 TEM images of the several CdS_xSe_{1-x} ($0 < x < 1$) nanorods, **a** $CdS_{0.8}Se_{0.2}$, **b** $CdS_{0.5}Se_{0.5}$, **c** $CdS_{0.2}Se_{0.8}$. **d** High-resolution TEM image of an individual CdS_xSe_{1-x} nanorod. The inset figure in **d** shows the selected area electron diffraction pattern

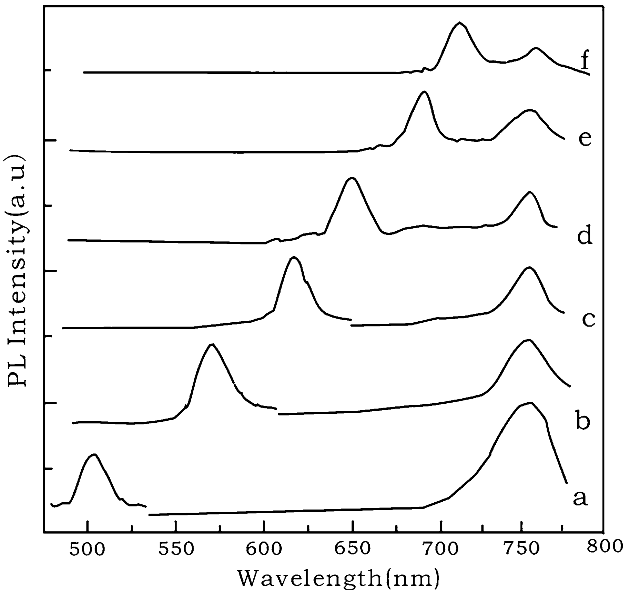

Fig. 4 PL spectra of a series of CdS_xSe_{1-x} nanorods with different x values (a) 1.0; (b) 0.80; (c) 0.60; (d) 0.40; (e) 0.20; (f) 0. All the samples were excited with 405 nm excitation wavelength at room temperature

energy feature is associated with the deep level transitions. It is found that, for the CdS_xSe_{1-x} nanorods, the PL peak associated with the neat band edge recombination continuously blue shifts with the x value increasing. The typical full width at half-maximum (fwhm) of the band-edge PL of these nanorods is ~25 nm, which is comparable to those of the widely used II-VI spherical quantum dots [17]. Such narrow peaks of the band-edge fluorescent emission also imply that the distribution of the composition of these CdS_xSe_{1-x} nanorods is quite uniform. In particular, the PL intensity of the low energy band can be considered as an indication of the defect density or structure disorder introduced in the nanorods during the growth process: i.e., the higher the PL intensity of the low energy band with respect to the NBE band, the higher the structural disorder. Meanwhile, it is also found that, with the ratio of Se to S enhancing, the PL intensity of the band-gap transition increases, in contrast to the decrease of the PL intensity originating from the anionic antisite defects.

The formation of the CdS_xSe_{1-x} nanorods can be attributed to the chemical solution transport growth mechanism.

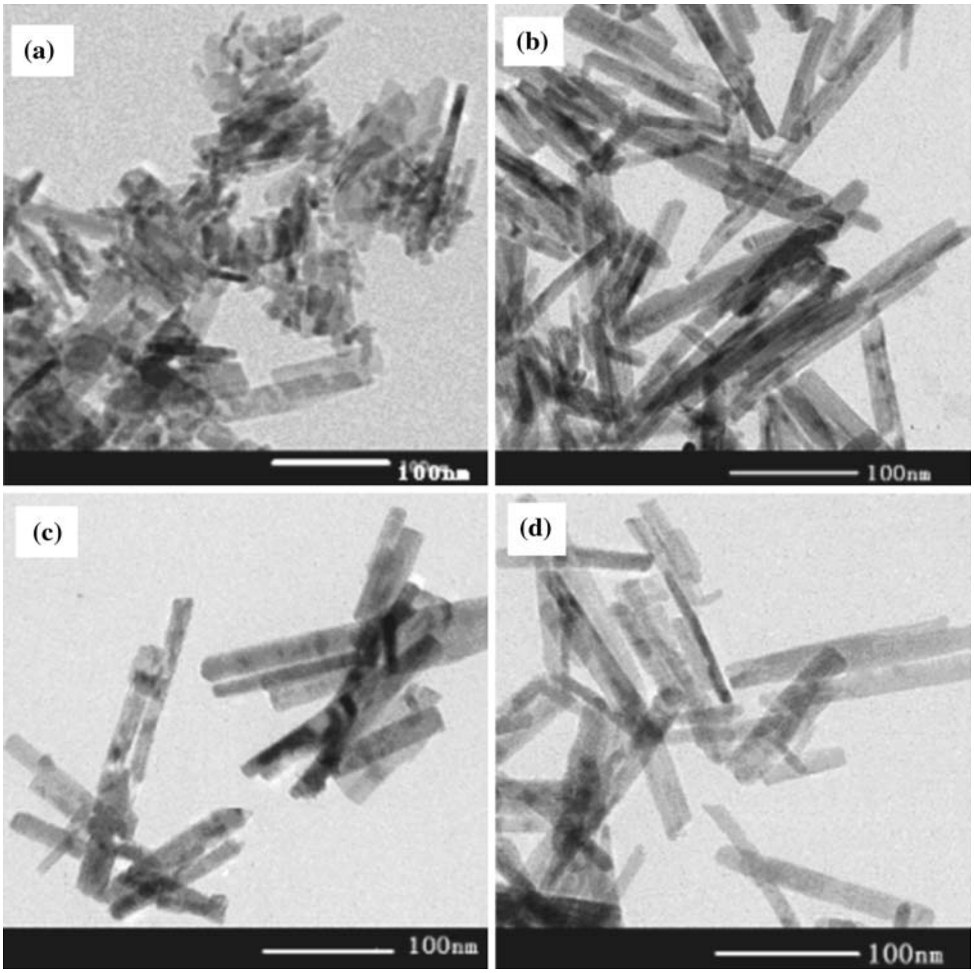

Fig. 5 TEM images of the $CdS_{0.5}Se_{0.5}$ nanocrystals prepared at 180 °C with different sulfur precursor. **a** Na_2S as sulfur precursor, **b** CS_2 as sulfur precursor, **c** CH_3CSNH_2 as sulfur precursor, **d** NH_2CSNH_2 as sulfur precursor

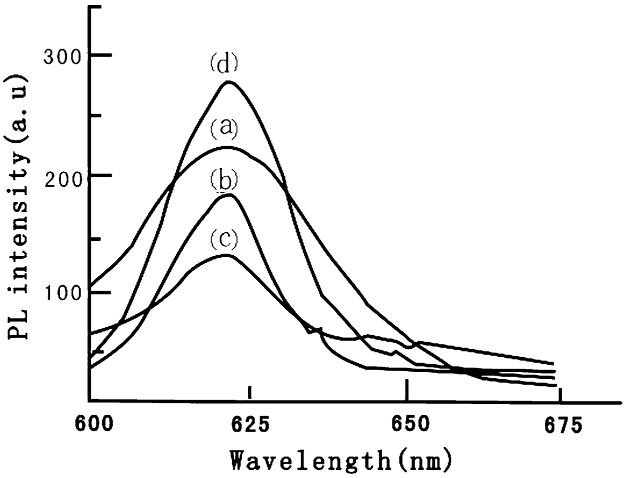

Fig. 6 PL spectra of $CdS_{0.5}Se_{0.5}$ nanocrystals with different sulfur precursor under excitation at 405 nm. (a) Na_2S as sulfur precursor, (b) CS_2 as sulfur precursor, (c) CH_3CSNH_2 as sulfur precursor, (d) NH_2CSNH_2 as sulfur precursor

[18, 19] In a typical synthetic system, the PEG2000 plays an important role in 1D growth of CdS_xSe_{1-x} nanorods. Cd^{2+} ions are well dispersed in the polymer matrix. Meanwhile, ethylenediamine is a strongly bidentatig solvent, readily chelating divalent cadmium ions [20].The polymer may be connected with the ethylenediamine to form chain structures with many pores, which are coterminous and continuous. Therefore, during the formation of the CdS_xSe_{1-x} nanorods, PEG2000 gel serves as a molecular template in control of the CdS_xSe_{1-x} nanorods growth.

To figure out the relationship between the reactants and the crystal structure, Na_2S, CS_2, CH_3CSNH_2, and NH_2CSNH_2 were substituted as the sulfur precursor for the synthesis of $CdS_{0.5}Se_{0.5}$ nanostructures, respectively. Figure 5 shows the TEM images of the sample obtained at 180 °C with various sulfur sources. It can be seen that irregular shorter and thicker nanorods together with nanoparticles is dominated in the samples (Fig. 5a), with Na_2S substituted for sulfur as the precursor. Meanwhile, when CS_2, CH_3CSNH_2, and NH_2CSNH_2 were adopted as sulfur source, the regular nanorods were also obtained (Fig. 5b, c, and d), indicating the polymer-controlled growth strategy suitable for synthesized CdS_xSe_{1-x} nanocrystals with different sulfur precursors.

Figure 6 shows the PL emission spectrum of the $CdS_{0.5}Se_{0.5}$ obtained with different sulfur source. The spectra of all samples show a single emission peak corresponding to NBE recombination at 623 nm.

Conclusion

Alloyed ternary CdS_xSe_{1-x} nanorods have been synthesized by the thermal treatment of Cd^{2+} dispersed PEG2000 gel with ethylenediamine solution of sulfur and selenium in a sealed system at 180 °C for 24 h. The lattice constant c of the ternary alloy varies linearly with the chemical composition x, according to the Vegard's rule. A possible mechanism for the formation of the CdS_xSe_{1-x} nanorods can be explained by the chemical solution transport growth mechanism. PL measurements show that all the CdS_xSe_{1-x} nanorods have a stronger emission band near their band edges, and these peaks could shift towards to high energy as the S ratio in the CdS_xSe_{1-x} enhanced. This may provide possibilities of developing a variety of ternary or quaternary semiconductor nanorods based on II-IV and II-V materials. With broadly tunable optical and electrical properties, these alloyed nanorods could result in significant applications in the tunable nano/micro photoelectric devices in the visible region.

References

1. Gudiksen MS, Lieber CM (2000) J Am Chem Soc 122:8801
2. Gudiksen MS, Wang J, Lieber CM (2002) J Phys Chem B 106:4036
3. Ma DDD, Lee CS, Au FCK, Tong SY, Lee ST (2003) Science 299:1874
4. Huang MH, Mao S, Feick H, Yan H, Wu Y, Kind H, Weber E, Russo R, Yang P (2001) Science 292:1897
5. Choi HJ, Johnson JC, He R, Lee SK, Kim F, Pauzauskie P, Goldberger J, Saykally RJ, Yang P (2003) J Phys Chem B 107:8721
6. Duan X, Huang Y, Agarwal R, Lieber CM (2003) Nature 421:241
7. Zhong X, Feng Y, Knoll W, Han M (2003) J Am Chem Soc 125:13559
8. Bailey RE, Nie S (2003) J Am Chem Soc 125:7100
9. Petrov DV, Santos BS, Pereira GAL, Donega CDM (2002) J Phys Chem B 106:5325
10. Kulkarni SK, Winkler U, Deshmukh N, Borse PH, Fink R, Umbach E (2001) Appl Surf Sci 169:438
11. Perna G, Pagliara S, Capozzi V, Ambrico M, Ligonzo T (1999) Thin Solid Films 349:220
12. Meit G (1992) J Phys Condens Matter 4:7521
13. Jang E, Jun S, Pu L (2003) Chem Commun 24:2964
14. Ionov L, Sapra S, Synytska A, Rogach AL, Stamm M, Diez S (2006) Adv Mater 18:1453
15. David C, Michael C (2006) Infrared Phys Techn 48:227
16. Vegard L, Zeit F (1921) Physik 5:17
17. Qu LH, Peng XG (2002) J Am Chem Soc 124:2049
18. Zhang JH, Yang XG, Li SD, Wang DW, Xie Y, Qian YT (2000) J Cryst Growth 220:231
19. Zhang JH, Yang XG, Wang DW (2000) Adv mater 12:1348
20. Shelrick WS, Wachhold M (1997) Angew Chem Int Ed Engl 36:206